Formation of Electrostatic Interactions on the Protein-Folding Pathway

Mikael Oliveberg and Alan R. Fersht*

Cambridge Centre for Protein Engineering, Hills Road, Cambridge CB2 2QH, England, U.K.

Received May 1, 1995; Revised Manuscript Received September 1, 1995[⊗]

ABSTRACT: We describe a novel method of obtaining information about the structures of transient conformations on the folding pathway from their ionization equilibria: the H^+-titration behavior of a protein residue is determined in detail by its environment. We follow the consolidation of electrostatic interactions in the folding process by comparing the acid-titration behavior of four conformations on the folding pathway of barnase: the denatured state (**D**); the folding intermediate (**I**); the major transition state (‡); and the native state (**N**) in the scheme **D** ⇄ **I** ⇄ ‡ ⇄ **N**. The results show that strong electrostatic interactions are present in the major transition state: some of its carboxylate groups display the highly anomalous pK_A values of <2 that are found in **N**. However, the network of ionic surface interactions is not formed in ‡, and the overall protection of titrating residues is weakened. The results are consistent with the transition state being an expanded form of the native state, with a weakened but poorly hydrated core and a loosened periphery. The surface residues in such an expanded conformation are, on average, farther apart than are those in the center of the molecule. The results concerning the folding intermediate are less clear cut. We show that the interpretation of kinetic data relating to folding intermediates depends critically on assumptions about their equilibrium with other denatured states. We have, however, characterized the pH and ionic strength dependence of an apparent stability of **I**, using the deviation from two-state folding behavior, which can be used to investigate electrostatic properties of folding intermediates from a variety of mechanisms. In general, the data imply that **I** is somewhat similar to ‡. Apparently odd titration properties of **I** are investigated further in the accompanying paper [Oliveberg, M., & Fersht, A. (1996) *Biochemistry 35*, 2738−2749]. The approach in this study may be of particular use in testing theoretical results since the relationship between H^+-titration properties and protein structure can be treated by classical electrostatics.

The pK_A values of amino acids in proteins are determined in detail by the physical nature of their environment (Warshel & Åqvist, 1991). Upon folding of a protein, the residues are transferred from a solvent-exposed location in the denatured state (Tanford, 1968; Dill & Shortle, 1991), through a series of gradually consolidated conformations (Kuwajima, 1989; Creighton, 1992; Matouschek *et al.*, 1992; Serrano *et al*., 1992) to finally a specific position in the well-defined matrix of the native protein (Thornton, 1992). The titration property of an individual residue varies during this process, and its detailed behavior reports on the series of events on the folding pathway leading to the unique folded structure. Although a great deal is known about the ionization of native proteins [see, for example, Antosiewicz *et al.* (1993)], and to some extent about the ionization of the denatured state (Roxby & Tanford, 1971; Oliveberg *et al.*, 1995), there have been few, if any, reports on the titration properties of (transient) conformations in the folding pathway. An exception to this may be the extensive investigations of so called molten globules, which are ground states which, it is proposed, represent universal folding intermediates (Kuwajima, 1989; Ptitsyn *et al.*, 1990). The molten globules have been observed under equilibrium conditions for an increasing number of proteins and are characterized as compact "liquid-like" conformations involving various degree of secondary interactions but without fixed tertiary interactions (Ptitsyn, 1992). Typically, these states are induced by adding salt to acid-denatured proteins but can also be induced by decreasing the pH further below the acid-unfolding transition (Goto & Fink, 1989; Goto et al., 1990; Goto & Nishikiori, 1991). This behavior suggests that the denatured state involves a significant portion of charge repulsions (Oliveberg *et al.*, 1994, 1995), and when these interactions are decreased by solvent ions, the denatured state reaches a new, more compact structural equilibrium (Stigter & Dill, 1990). It is likely that the molten globules in these cases have titration properties resembling those of the more extended denatured state. The molten globule of carbonic anhydrase, however, unfolds at low pH (Wong & Hamlin, 1974), implying that this molten globule has titration properties different from those of the denatured state. Considering theoretical studies, which predict the existence of "dry", "wet", and "swollen" molten-globule states (Finkelstein & Shakhnovich, 1989), it is tempting to speculate that the molten globule of carbonic anhydrase involves a structured core [cf. Matouschek *et al.* (1992)] or elements of nonhydrated secondary structure (Griko *et al.*, 1994) that can significantly perturb the pK_A values of its carboxylate residue(s), whereas the former examples are liquid-like (hydrated?) states in which specific electrostatic interactions are reduced to a minimum.

The high-energy transition state, which precedes the formation of the native protein, contains significant native-like tertiary interactions (Serrano *et al.*, 1992). In agreement with experimental observations [see also Sugihara and Segawa (1984)], theoretical studies suggest that the transition state is an expanded form of the native state in which a

* To whom correspondence should be addressed.

[⊗] Abstract published in *Advance ACS Abstracts,* February 1, 1996.

0006-2960/96/0435-2726$12.00/0

significant part of the van der Waals energy is lost, but the degree of expansion is insufficient to permit rotational isomers of the side chains or penetration of water (Shakhnovich & Finkelstein, 1989).

In this paper we use a kinetic/thermodynamic approach to determine experimentally the titration behavior of the major transition state and folding intermediate of barnase (EC 3.1.27.3), a small ribonuclease from *Bacillus amyloliquefaciens* (Mauguen *et al.*, 1982).

EXPERIMENTAL PROCEDURES

Materials. Barnase was overexpressed and purified from *Escherichia coli* as described by Serrano and Fersht (1989). The buffers used were 50 mM glycine and HCl (pH 1.5−3.0), 50 mM sodium formate/formic acid (pH 2.7−4.2), 50 mM sodium acetate/acetic acid (pH 3.7−5.3), and 50 mM 2-(*N*-morpholino)ethanesulfonic acid (MES) (pH 6.3). HCl/KCl was used between pH 1.5 and 0.2. The ionic strength (μ)[1] was controlled with KCl. All chemicals were of analytical grade and purchased from Sigma.

Stopped-Flow Experiments. The unfolding and refolding of barnase were induced by pH jump by rapid mixing, using an Applied Photophysics DX-17 MV stopped-flow spectrofluorimeter. The instrument was connected to a thermostated water bath which maintained the temperature of the reservoir syringes and the observation cell within ±0.1 °C. The instrument was set up to mix the protein solution with unfolding and refolding buffer solutions in a volumetric ratio of 1:1, yielding a final protein concentration of 8 μM and a final buffer concentration of 50 mM. The intrinsic fluorescence of barnase decreases when the protein denatures, which allows unfolding and refolding transitions to be monitored by changes in fluorescence. Excitation was at 280 nm, and the emission was monitored at wavelengths greater than 315 nm, using a cut-off filter.

The stopped-flow experiments in this study can be divided into three classes: (i) studies of the pH dependence of the unfolding rate constant (k_u[pH]), where the native protein, dissolved in pure water, was mixed with acidic buffers into denaturing conditions, typically in the range of pH 3−0.2; (ii) studies of the pH dependence of the (apparent) refolding rate constant (k_f^{app} [pH]), where the denatured protein, dissolved in 32 mM HCl (pH 1.5), was mixed with buffers into refolding conditions at higher pH values, typically between pH 2 and 6.3; and (iii) double-jump, or sequential mixing experiments, where the protein was mixed with buffers in two consecutive steps—first, the denatured protein (in 32 mM HCl) was mixed with a refolding buffer into a 115 μL "delay loop", then the refolding reaction was allowed to proceed for a certain time (the delay time, 10−500 ms) and finally the contents of the delay loop were mixed with a second buffer back into denaturing conditions at a lower pH. The double-jump approach was used to study the unfolding kinetics of transient folding intermediates which were accumulated in the delay loop during the delay time. Salt was included in the syringes containing the refolding/unfolding buffer in order not to perturb the initial state of the protein, i.e., to avoid second-order effects such as polymerization or aggregation processes.

[1] Abbreviations: μ, ionic strength.

Data Analysis. The rate constants and amplitudes of the folding events were obtained by fitting a sum of exponential functions to the acquired data, using the data-analysis program Kaleidagraph (Adelbeck Software). In some cases a linear slope was included in the exponential expression to account for machine drift or photolysis. When processing the results mathematically, e.g., a series of closely spaced rate constants vs pH, a "smooth function" (Kaleidagraph) was fitted to the data, and this smooth function was then used to represent the experimental values mathematically.

Extrapolation of Stopped-Flow Data Obtained at High Temperatures to 25 °C. In order to study the unfolding kinetics in regions of pH where only the native state is populated at 25 °C, unfolding experiments were carried out at higher temperatures, 40 and 47.5 °C. At these temperatures the midpoint for the unfolding transition occurs above pH 4 (Oliveberg & Fersht, 1995), and consequently the unfolding rate constant [k_u(pH)] can be followed from about pH 3.5 and downward. k_u(pH) obtained from these experiments, however, has to be extrapolated to the reference temperature, 25 °C, using its temperature dependence. The temperature dependence of k_u(pH) is described by transition state theory

$$k_u(\mathrm{pH}) = \frac{k_B T}{h} e^{(-\Delta G^{\ddagger}(\mathrm{pH})/RT)} \quad (1)$$

where k_B is Boltzmann's constant, h is Planck's constant, T is the absolute temperature, R is the gas constant, and $\Delta G^{\ddagger}$(pH) is the (pH dependent) activation energy, which is here the difference in free energy between the native state and the transition state of unfolding. Using the thermodynamic identity $\Delta G^{\ddagger}(\mathrm{pH}) = \Delta H^{\ddagger}(\mathrm{pH}) - T\Delta S^{\ddagger}(\mathrm{pH})$, where $\Delta H^{\ddagger}$(pH) is the activation enthalpy and $\Delta S^{\ddagger}$(pH) is the activation entropy, eq 1 can be rewritten:

$$\ln\left(\frac{k_u(\mathrm{pH})}{T}\right) = \ln\left(\frac{k_B}{h}\right) + \frac{\Delta S^{\ddagger}(\mathrm{pH})}{R} - \frac{\Delta H^{\ddagger}(\mathrm{pH})}{RT} \quad (2)$$

The value of $\Delta H^{\ddagger}$(pH) at each pH was obtained from the slope of the corresponding Eyring plots [$\ln(k_u/T)$ vs $(1/T)$] (Figure 3). The values of $\Delta H^{\ddagger}$(pH) were plotted versus pH and a linear function [$\Delta H^{\ddagger}(\mathrm{pH}) = \alpha + \beta\mathrm{pH}$] was fitted to the plot (Figure 3). This function was then used to represent $\Delta H^{\ddagger}$(pH) in eq 3. To obtain an expression for the extrapolation of k_u(pH) from any temperature (T) to 298.15 K (25.0 °C), eq 2 was divided by the corresponding expression for k_u(pH) at T = 298.15 °K, which gives

$$\log k_u^{298.15}(\mathrm{pH}) = \log k_u^{T}(\mathrm{pH}) - \frac{1}{2.3}\left[(\alpha + \beta\mathrm{pH})\left(\frac{1}{T} - \frac{1}{298.15}\right) - \ln\left(\frac{298.15}{T}\right)\right] \quad (3)$$

Equations 2 and 3 assume the change in heat capacity (ΔC_p) between the native protein and the transition state to be negligible and, hence, $\Delta H^{\ddagger}$ and $\Delta S^{\ddagger}$ to be independent of temperature. It follows that the plots of $\ln(k_u/T)$ versus $(1/T)$ are linear, which is consistent with the observed unfolding kinetics (cf. Figure 3). In cases when the Eyring plot is found to be curved, $\Delta C_p \neq 0$ and eq 2 has to be modified to include the temperature dependence of $\Delta H^{\ddagger}$ and

$\Delta S^{\ddagger}$ [see eq 6 in the accompanying paper (Oliveberg & Fersht, 1995)].

Relationship between the pH Dependence of $\Delta G_{A/B}$ and the Difference in Degree of Protonation of the Protein States A and B. It can be shown from the law of mass action that the difference in number of bound protons between two protein conformations, A and B, is related to the pH dependence of the free-energy difference between these conformations (Tanford, 1968, 1970):

$$\frac{\partial[\Delta G_{\text{A-B}}(\text{pH})]}{\partial(\text{pH})} = 2.3RT[Q_{\text{A}}(\text{pH}) - Q_{\text{B}}(\text{pH})] = 2.3RT\Delta Q_{\text{A-B}}(\text{pH}) \quad (4)$$

where $\Delta G_{\text{A-B}}$ is the difference in free energy between state A and B. Q_{A}(pH) and Q_{B}(pH) are the number of protons bound to state A and B, respectively, and $\Delta Q_{\text{A-B}}$(pH) the change in the number of protons taken up on the transition from B to A.

Since the first-order rate constants for the unfolding/folding process are related to the free-energy difference between the native/denatured state and the major transition state according to (eq 1), the pH dependence of log k_{u}(pH)/log k_{f}(pH) is directly proportional to the pH dependence of $\Delta G_{\ddagger\text{-N}}$(pH)/$\Delta G_{\ddagger\text{-D}}$(pH) and can, hence, be related to changes in protonation, for example,

$$\frac{\partial \log k_{\text{u}}}{\partial \text{ pH}} = -\frac{1}{2.3RT}\frac{\partial \Delta G^{\ddagger}}{\partial pH} = -\Delta Q_{\ddagger\text{-N}}(\text{pH}) \quad (5)$$

RESULTS

Nomenclature of Rate Constants. The rate constant obtained from the fit of an exponential expression to stopped-flow refolding data is referred to as the observed refolding rate constant, or $k_{\text{f}}^{\text{obs}}$. Analogously, the rate constant obtained from the time course of unfolding is referred to as the observed unfolding rate constant, or $k_{\text{u}}^{\text{obs}}$. Since $k_{\text{f}}^{\text{obs}}$ and $k_{\text{u}}^{\text{obs}}$ yield the same value if they are measured under the same final conditions, for example at the midpoint for the unfolding transition (Figure 2), it is sometimes practical to refer simply to the observed rate constant, or k^{obs}, which can then be either $k_{\text{f}}^{\text{obs}}$ or $k_{\text{u}}^{\text{obs}}$. The observed rate constant (k^{obs}) for equilibration of the reaction A $\rightleftharpoons$ B is always the sum of the forward and reverse rate constants, in this case

$$k^{\text{obs}} = k_{\text{f}}^{\text{app}} + k_{\text{u}} \quad (6)$$

where k_{u} is the unfolding rate constant which corresponds to the free-energy difference between the native state and the transition state for unfolding (cf. eq 1), and $k_{\text{f}}^{\text{app}}$ is the refolding rate constant which correspond to the apparent free-energy difference between the denatured ground state and the transition state for refolding. $k_{\text{f}}^{\text{app}}$ is denoted *apparent* since it may not always refer to the same ground state as this may vary with pH (see Appendix).

Unfolding Kinetics at 25 °C. The time-resolved unfolding of barnase with pH displays typically a first-order monophasic decrease in fluorescence (Figure 1). The time course for unfolding this major phase shows a pronounced pH dependence. At lower pH values, the observed unfolding rate constant increases approximately exponentially with decreasing pH, and the increase shows little tendency to level off within the pH region observed experimentally (top panel, Figure 2). Above pH 2, at the beginning of the transition region, the pH dependence appears to decrease and even to display a minimum at the transition midpoint. This curvature, however, does not necessarily imply any change in the pH dependence of the kinetics *per se* but is a consequence of the observed rate constant (k^{obs}) representing, under all conditions, the sum of the unfolding and refolding rate constants (k_{u} and $k_{\text{f}}^{\text{app}}$, eq 6): in the transition region where both the native and the denatured protein are present under equilibrium conditions, k_{u} and $k_{\text{f}}^{\text{app}}$ are of similar magnitude and, hence, both contribute to the observed rate constant (eq 6).

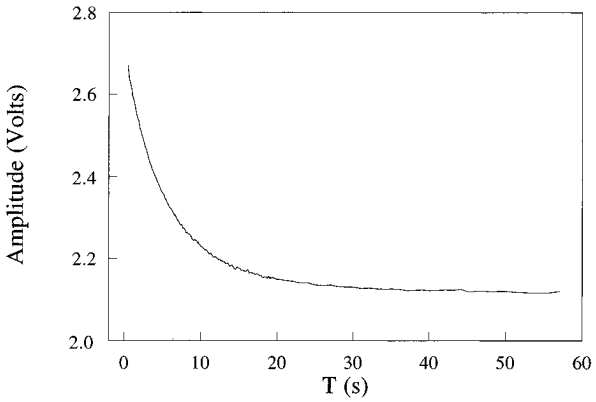

FIGURE 1: Transient fluorescence change of barnase upon acid unfolding at pH 2 and low ionic strength. Rapid mixing was achieved by stopped-flow. Excitation was at 280 nm, and the fluorescence was detected above 315 nm using a cut-off filter. The unfolding reaction displays typically a monophasic decay, but within the transition region an additional slower phase (corresponding to *trans* → *cis* isomerizations around the peptidyl−prolines in the unfolded state) is resolved.

At pH values close to the midpoint of the unfolding transition (around pH 2.2 at μ = 200 mM), an additional slower unfolding phase can be resolved (top panel, Figure 2). This second relaxation ($k_{\text{u}}^{\text{iso}}$), which appears independent of pH, is caused by *trans* → *cis* isomerizations of peptidyl−proline bonds in the denatured state and occurs when the final conditions result in an equilibrium between native and denatured protein (Kiefhaber *et al.*, 1992). Consistently, the rate constant for this phase is of similar magnitude to that observed previously for isomerizations of peptidyl−proline bonds (Matouschek *et al.*, 1992) and to that resolved in the refolding kinetics, at 0.04 s^{-1} (see below).

The pH dependence of the major unfolding rate constant, as well as its absolute value, decreases upon addition of salt (middle panel, Figure 2). The slow *trans* → *cis* peptidyl-proline phase cannot be resolved with sufficient accuracy at high ionic strength, since the protein under these conditions undergoes an aggregation, or polymerization, process in this time scale [see accompanying paper (Oliveberg & Fersht, 1996)].

The bottom panel of Figure 2 shows the amplitude of the fluorescence decrease upon transient unfolding plotted versus pH. The amplitudes, which are linked to the extent of unfolding at each pH, correspond to the fluorescence change obtained from titration of the protein with acid under equilibrium conditions [cf. Oliveberg *et al.* (1995)]. To compare the kinetic amplitudes directly with equilibrium data, however, the sum of the major amplitude and the smaller *trans*−*cis* amplitude must be used.

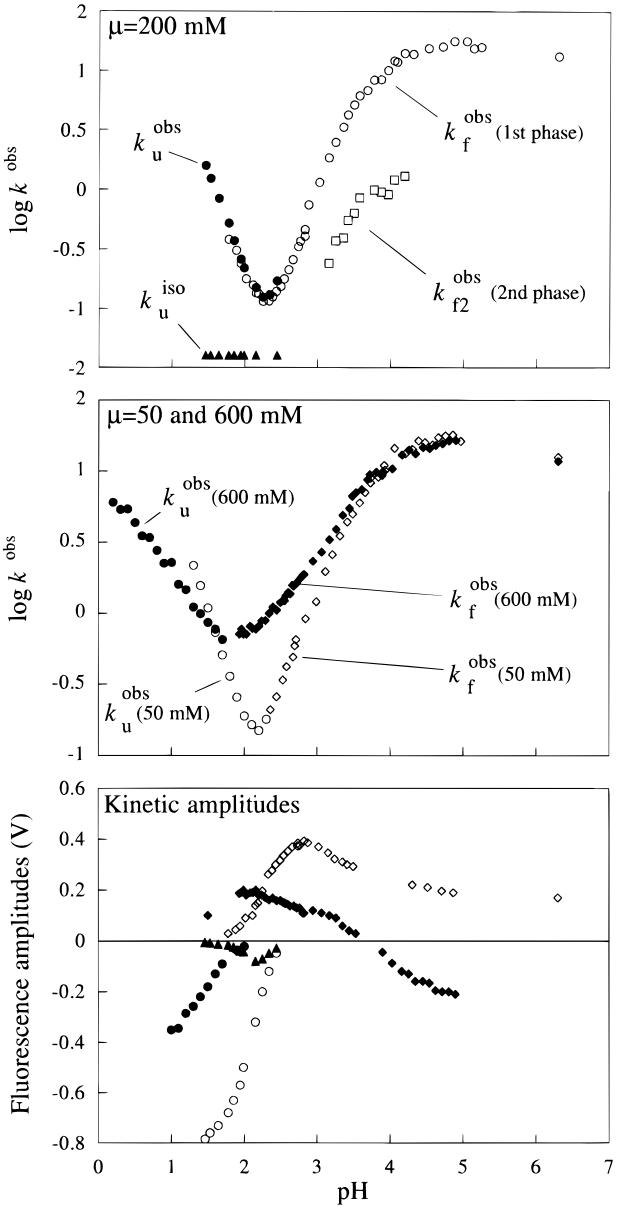

FIGURE 2: pH dependence of the unfolding and refolding kinetics of barnase at different ionic strengths (μ). k^{obs} has units of s^{-1}. (Top panel) μ = 200 mM, (●) the rate constant of the major unfolding phase; (▲) the rate constant of the slow unfolding phase (k_u^{iso}); (○) the observed rate constant of the first major refolding phase (k_f^{obs} first phase); (□) the rate constant of the intermediate refolding phase (k_{f2}^{obs} second phase). In a relaxation process A ⇄ B the observed rate constant is always the sum of the forward and reverse rate constants. Hence, the observed rate constants of the major unfolding phase (k_u^{obs}) and the major refolding phase (k_f^{obs} first phase) show the same values around the pH for the transition midpoint (pH 2.3), where the unfolding and the refolding relaxation can be studied under the same final conditions. (Middle panel) (open symbols) μ = 50 mM and (closed symbols) μ = 600 mM. (○) The rate constant for the major unfolding phase, μ = 50 mM (k_u^{obs} 50 mM); (◇) the rate constant for the major refolding phase, μ = 50 mM (k_f^{obs} 50 mM). (●) The rate constant for the major unfolding phase, μ = 600 mM (k_u^{obs} 600 mM); (◆) the rate constant for the major refolding phase, μ = 600 mM (k_f^{obs} 600 mM). (Bottom panel) The fluorescence amplitudes associated with the rate constants in the middle panel. (○) The major unfolding amplitude for k_u^{obs} (50 mM); (▲) the amplitude for the slow unfolding phase, k_u^{iso} (μ = 200 mM, top panel); (◇) The refolding amplitude for k_f^{obs} (50 mM); (●) the unfolding amplitude for k_u^{obs} (600 mM); (◆) the refolding amplitude for k_f^{obs} (600 mM).

Refolding Kinetics at 25 °C. The three peptidyl−prolyl bonds in the native state of barnase are all *trans*, whereas about 20−30% of the unfolded state has a *cis* peptidyl−prolyl bond. The major amplitude in the kinetics of refolding relates to the rapid interconversion of the *all-trans* states. The denatured conformations containing a *cis* peptidyl−proline fold much more slowly, rate limited by the *cis*−*trans* isomerization. Accordingly, the refolding of barnase displays typically three distinct phases: a first, major phase, which constitutes about 80% of the total refolding amplitude; and the two slower phases of about 10% each, which relate to *cis* → *trans* isomerizations around the prolines (Matouschek *et al.*, 1992).

The pH dependence of the major refolding phase displays an increasing rate constant with increasing pH (top and middle panel, Figure 2). Around pH 4, however, the pH dependence levels off, so that k_f^{obs} reaches a maximum of about 16 s^{-1} around pH 5. At pH 6.3, the highest pH used in this study, k_f^{obs} =13 s^{-1}, consistent with earlier observations (Matouschek *et al.*, 1992). In the transition region, k_f^{obs} converges with the rate constant observed in the unfolding experiments (cf. eq 6). The intermediate refolding phase, with a rate constant of around 1 s^{-1}, shows a pH dependence similar to that of the main refolding phase. This phase has previously been attributed to a *cis* → *trans* isomerization event, and the pH dependence found here implies that this is coupled with higher-order structural changes. The slowest refolding phase, with a rate constants of about 0.04 s^{-1}, appears independent of pH (data not shown).

At pH values above 3.5, there is no observable dependence of the rate constants on ionic strength (μ). At lower pH values, however, the rate constant of the major refolding phase increases in the presence of salt and its pH dependence becomes less pronounced (middle panel, Figure 2). It is seen in the middle panel of Figure 2 that, as for the transition midpoint (Oliveberg *et al.*, 1994), the minimum of the plot log(k^{obs}) versus pH occurs at a lower pH value at high ionic strength than at low ionic strength. At μ = 50 mM, the minimum of log(k^{obs}) occurs precisely at the transition midpoint, whereas at μ = 600 mM the minimum of log(k^{obs}) occurs at a pH slightly higher than that observed for the transition midpoint (cf. Figure 8).

At μ = 50 mM, the major refolding phase is observed as an increase in fluorescence when using a 315 nm cut off filter (bottom panel, Figure 2). The refolding amplitude reaches a maximum around pH 3, and above this pH the amplitude decreases to reach only half the maximum value at pH 6.3. The behavior is not related to the final occupancy of the native state, since the protein is completely folded above pH 3. Instead, the variation can be traced to an increasing fluorescence of the denatured state: the effect is most clear at μ = 600 mM, where the fluorescence of the denatured state becomes stronger than that of the native state just below pH 4. As a result, the amplitude of the refolding reaction inverts above pH 4 (bottom panel, Figure 2). Hence, the refolding kinetics has to be monitored with a set of different optical filters around pH 4, where the refolding amplitude would otherwise become too small to allow accurate determination of the rate constant. The filters used were 315 nm, 335 nm cut-off filters and a 320−380 band-pass filter.

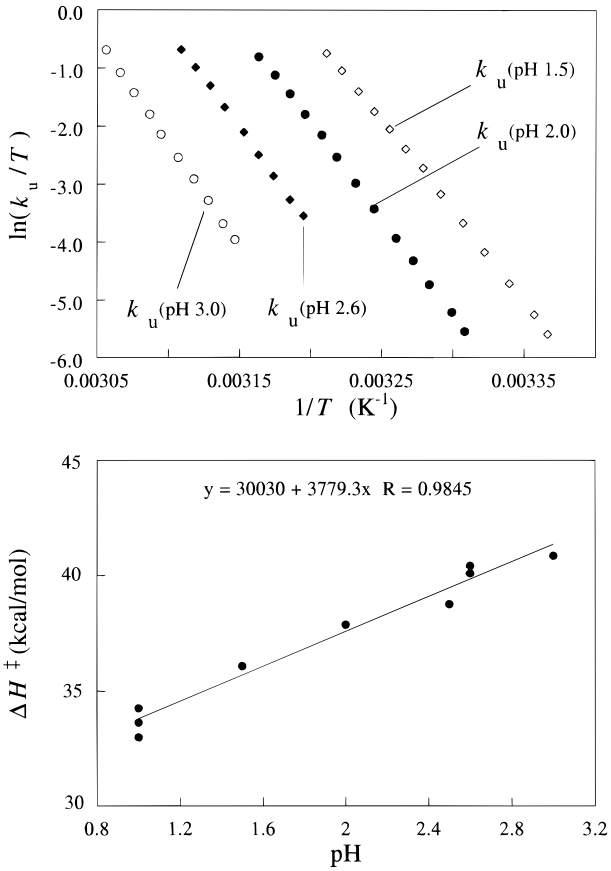

FIGURE 3: Temperature dependence of the unfolding rate constant of barnase as a function of pH. k_u has units of s^{-1}. (Top panel) Eyring plots of the unfolding rate constant at pH 1.5 (◇), pH 2.0 (●), pH 2.6 (◆), and pH 3.0 (○). (Lower panel) The activation enthalpy of the unfolding rate constant plotted versus pH. A linear function was fitted to the data and then used to represent $\Delta H^{\ddagger}$(pH) in temperature extrapolations by eq 3 (Figure 4). The plot includes data from both μ = 50 mM and μ = 600 mM, since $\Delta H^{\ddagger}$ was found to be independent of ionic strength.

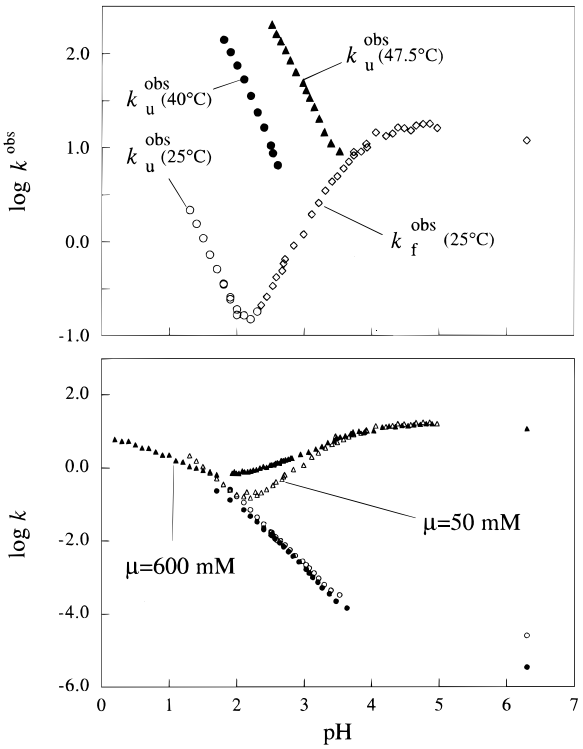

FIGURE 4: pH dependence of the unfolding rate constant under refolding conditions, extrapolated from elevated temperatures. k_u has units of s^{-1}. (Top panel) μ = 50 mM. The pH dependence of the unfolding rate constant obtained at 47.5 °C (▲) and 40 °C (●), compared with the unfolding rate constant at 25 °C (○) and the refolding rate constant at 25 °C (◇). (Lower panel) The complete set of unfolding/refolding rate constants at 25 °C, μ = 50 mM (open symbols) and μ = 600 mM (closed symbols). The observed rate constant at 25 °C at μ = 50 mM (△) and μ = 600 mM (▲), the unfolding rate constants from the top panel which have been extrapolated to 25 °C at μ = 50 mM (○) and corresponding data from μ = 600 mM (●) (see text and Figure 3). The unfolding rate constants at pH 6.3 were obtained by urea-jump experiments (see text and Figure 5).

Unfolding Kinetics Recorded at High Temperatures and Extrapolated to 25 °C. In order to determine the pH dependence of the unfolding rate constant under folding conditions, the unfolding reaction was determined at temperatures above the melting point of the protein and then extrapolated to 25 °C. Figure 3 shows the Eyring plot of the unfolding rate constant at pH values between 1.0 and 3.0. The activation enthalpies ($\Delta H^{\ddagger}$) obtained from the slope of these graphs (eq 2) are plotted versus pH (Figure 3), and the pH dependence of $\Delta H^{\ddagger}$ was subsequently used to extrapolate the unfolding rate constants obtained at high temperatures to 25 °C (eq 3) (cf. Figure 4).

The unfolding kinetics observed at high temperatures displays a pH dependence similar to that at 25 °C, although the minimum of log(k^{obs}) occurs at a higher pH, and the rate of unfolding at this pH is faster. Figure 4 shows the unfolding rate constants obtained at 25, 40, and 47.5 °C compared with the refolding rate constant at 25 °C. Despite the use of refolding data obtained at a fixed lower temperature, the plot provides a representative approximation of the temperature dependence of log(k^{obs}) versus pH, since the refolding rate constant shows only a relatively small temperature dependence [accompanying paper (Oliveberg & Fersht, 1996)]. The data points obtained near the transition region were left out in the extrapolation to ensure that the observed rate constants are entirely dominated by k_u (eq 6). This could otherwise introduce an artificial curvature of log(k_u) versus pH. The validity of the extrapolation method is confirmed by the coincidence of extrapolated data with data obtained at 25 °C (around pH 1.9 at μ = 50 mM) and the coincidence of data extrapolated from two different temperatures (around pH 2.5).

It is seen in Figure 4 that although the unfolding rate constant decreases upon addition of salt at lower pH values, there is no salt-dependence observed between pH 2 and 3.5. At pH 6.3, however, the unfolding rate constant yet again decreases in the presence of salt. The refolding rate constant, on the other hand, is increased by the presence of salt at low pH but appears independent of ionic strength above pH 3.5. It is interesting to notice that the stability of barnase shows a salt-independent, isoenergetic point around pH 3.5 (Figure 8) (Oliveberg *et al.*, 1994).

Unfolding Rate Constant in Pure Water As Determined by Urea Unfolding at pH 6.3. In order to determine the unfolding rate constant (k_u) under conditions of maximum stability and high ionic strength, the unfolding kinetics was determined by stopped-flow fluorescence at various high concentrations of urea (4−8 M) in the presence of 600 mM KCl. The plot of log k_u versus [urea] for barnase and its mutants has been shown to display a slight downward

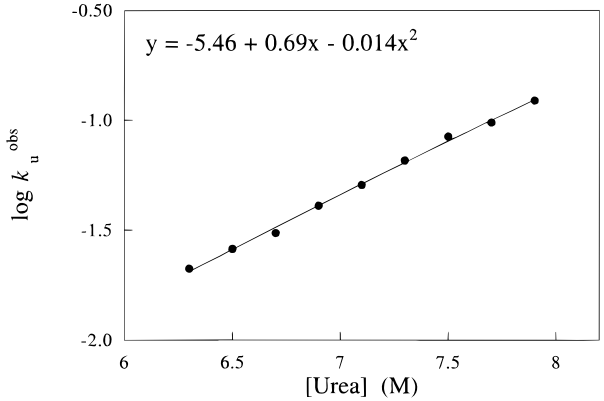

FIGURE 5: Urea dependence of the observed unfolding rate constant of barnase at pH 6.3, μ = 600 mM, obtained by urea-jump experiments. k_u has units of s^{-1}. The polynomial fit was used to calculate the unfolding rate constant at [urea] = 0 (eq 6).

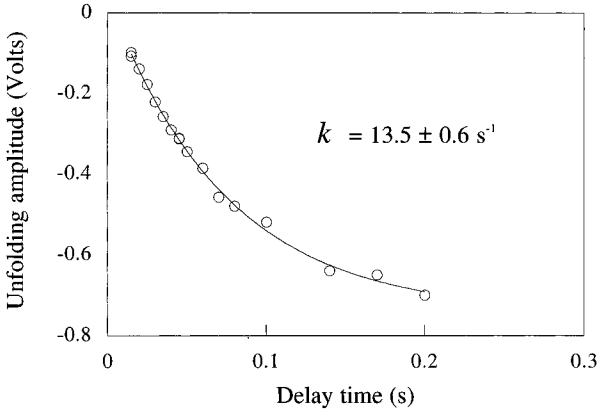

FIGURE 6: Unfolding amplitudes obtained from double-jump experiments as function of delay time. A solution of barnase at pH 1.5 was mixed with high-pH buffer and allowed to incubate at pH 6.3 for a variable time (the delay time) and then mixed with a second buffer to unfolding conditions at pH 1.5 where the unfolding kinetics were monitored. The exponential increase of the unfolding amplitudes versus delay time fits precisely the rate constant of refolding observed at pH 6.3, 13 s^{-1}, suggesting that the relaxation of the preequilibrium (see Figure 7) is too fast to be resolved by stopped-flow.

curvature according to

$$\log(k_u) = \log(k_u^0) + m_{ku}[\text{urea}] - 0.014[\text{urea}]^2 \quad (7)$$

where m_{k_u} is a variable that depends on mutation and experimental conditions, −0.014 is a parameter that defines the deviation from linearity (Matouschek *et al*., 1994), and k_u^0 is the unfolding rate constant in units of s^{-1} in the absence of urea [cf. Shortle and Meeker (1986)]. The value obtained for $\log(k_u^0)$ by eq 7 at μ = 600 mM is −5.46 ± 0.07 (m_{k_u} = 0.69) (Figure 5). At μ = 50 mM and pH 6.3, $\log(k_u^0)$ has previously been determined to −4.59 ± 0.07 (m_{k_u} = 0.65) (Sanz & Fersht, 1993).

Double-Jump Experiments at 25 °C. To ensure that the observed pH dependence is not induced or perturbed by changes of rate-limiting step (transition state), we tested our results by double-jump experiments. The unfolding rate constant observed at pH 1.5 in the double-jump experiments (i.e. after short incubation of the denatured protein under refolding conditions at pH 6.3 in the stopped-flow delay loop) is identical to that observed in the unfolding experiment above (Figure 2). No additional (fast) phase due to unfolding of a transiently accumulated folding intermediate can be resolved. The amplitude of the unfolding phase is proportional to the amount of renatured protein in the delay loop and increases exponentially with increasing delay time. A plot of the unfolding amplitude versus delay time at pH 6.3 (Figure 6) fits an exponential curve with a rate constant of 13.5 ± 0.6 s^{-1}. This rate constant is identical to that for the refolding reaction at pH 6.3. Double-jump experiments to final conditions of high ionic strength, or into the transition regions, revealed no additional phases, and the results are consistent with predictions from unfolding and refolding data in Figure 2.

DISCUSSION

The objective of this study is to determine the pH dependence of the stability of the various conformations in the folding pathway of barnase, and to use these data to determine how electrostatic interactions consolidate in the course of the folding process. In principle the analysis consists of three steps. The first step is to determine folding and unfolding rate constants and protein stability over as wide a pH range as possible. The second step is to combine these data to determine the pH dependence of individual equilibrium constants in the folding pathway (including the quasi-thermodynamic equilibria between ground states and transition barriers). This step requires careful consideration of the model for the folding pathway (cf. Scheme 1, below), and it is demonstrated in the Appendix how the number of folding intermediates and their relative stability affects the interpretation of refolding rate constants. Finally, the equilibrium constants are used to determine the H^+-titration behavior of the conformational species in the folding pathway by application of simple mass-action theory.

Comparison of the ionization equilibria between consecutive conformations in the folding pathway provides a novel method of obtaining information about their structures, and, perhaps more importantly, the approach constitutes a link to theoretical studies since the relationship between titration properties of ionizable residues and protein structure can be treated by classical electrostatics.

Model for the Folding Pathway of Barnase. It has been demonstrated previously that the refolding of barnase is not a two-state process but proceeds via transient accumulation of a folding intermediate (Matouschek *et al*., 1990; Bycroft *et al*., 1990). The kinetic evidence for this was obtained from urea denaturation experiments: in a two-state reaction, **D** ⇄ **N**, the equilibrium constant ($K_{D\text{-}N}$) is determined by the ratio of the reverse ($k_{N\to D}$) and forward ($k_{D\to N}$) rate constants

$$K_{D\text{-}N} = \frac{k_{N\to D}}{k_{D\to N}} \quad (8)$$

where ($k_{N\to D}$) and ($k_{D\to N}$) would correspond to the unfolding and refolding rate constants respectively; but with barnase, the observed rate constants give anomalous values, i.e., $K_{D\text{-}N} \neq k_u/k_f^{obs}$. At high urea concentrations (above 3 M), $K_{D\text{-}N} \approx k_f^{obs}/k_u$, but at lower concentrations of urea the urea dependence of k_f^{obs} starts to decrease, so that, in pure water, k_f^{obs} is only one hundredth of the value expected from k_u and $K_{D\text{-}N}$. The major folding reaction remains monophasic, and no additional relaxation can be resolved. From these observa-

tions, it was concluded that the kinetics in the absence of denaturant do not represent refolding from the unfolded state but from a more stable kinetic intermediate which is in rapid equilibrium with the unfolded state according to

Scheme 1

$$\mathrm{D} \overset{\text{fast}}{\rightleftharpoons} \mathrm{I} \underset{k_u = 2.6 \times 10^{-4}\ \mathrm{s^{-1}\ N}}{\overset{k_f = 13\ \mathrm{s^{-1}}}{\rightleftharpoons}}$$

where $\Delta G_{D\text{-}N} = 10-11$ kcal/mol at pH 6.3 and $\mu = 50$ mM (Johnson & Fersht, 1995) and $\Delta G_{D-I} = 2-3$ kcal/mol. Unfortunately, the values of k_u and $K_{D\text{-}N}$ cannot be measured directly in the absence of denaturant at 25 °C but have to be determined at high urea concentrations (>4.5 M for wild-type protein and >2−3 M for destabilized mutants) and subsequently extrapolated to pure water. Also, the determination of k_u in pure water relies on the assumption that the major transition state for unfolding remains the same at all concentrations of denaturant or changes uniformly with concentration of denaturant (cf. eq 7). In the present study, however, we confirm the observations from the urea experiments by providing an additional way of determining deviations from minimal two-state behavior—the dependence on pH.

Deviations from Two-State Behavior as Determined by Acid Denaturation. The double-jump experiments, in which the protein is allowed to refold for varying times and then is allowed to unfold (Figure 6), show that the interconversion between the unfolded state and any folding intermediate is fast and remains unresolved by stopped-flow also in the low-pH range. Even if the intermediate and the unfolded states were spectroscopically indistinguishable, a lag would appear in the plot of unfolding amplitudes versus delay time if $k_{D\to I}$ approaches $k_{I\to N}$, 13 s^{-1} (Figure 6).

Since the unfolding of any partly structured folding intermediates does not contribute to the observed unfolding kinetics, we suggest that the unfolding rate constant at all pH values [k_u(pH)] monitors changes in the free energy between the native protein (**N**) and the major transition state (‡) (Figure 7). The refolding rate constant expected from a two-state mechanism, i.e., the refolding rate constant which corresponds to the free-energy difference between **D** and ‡ [$k^{calc}_{D\to N}$(pH), Figure 7] can be calculated from the measured equilibrium constant for unfolding [$K_{D\text{-}N}$(pH), Figure 8] and k_u(pH) according to eq 8. The pH dependence of $k^{calc}_{D\to N}$ is shown in Figure 9. The coincidence of $k^{calc}_{D\to N}$ and k^{obs}_f at pH values below pH 2.5 reveals that barnase displays a two-state behavior in and below the transition region. At higher pH values, however, $k^{obs}_f < k^{calc}_{D\to N}$, implying that the observed refolding reaction under these conditions takes place from a protein conformation more stable than the denatured state observed in the thermal unfolding experiments (**D**) (Figure 7). To be consistent with earlier work, this apparently stabilized denatured conformation is referred to as the folding intermediate (**I**) (Scheme 1). In summary, it may be concluded from Figure 9 that the addition of acid changes the ground state of the refolding reaction from **I** to **D**.

Titration Behavior of the Native State and the Major Transition State. The titration by protons of the native state of barnase has been investigated in previous studies and can be summarized as follows (Oliveberg *et al.*, 1994, 1995). Of the 12 acidic residues of barnase, approximately eight become protonated between pH 3 and 4, the equivalent of

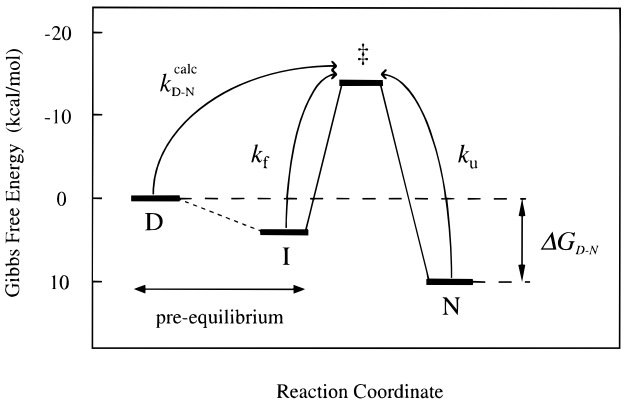

FIGURE 7: Free energy diagram showing the different conformations of barnase under refolding conditions at pH 6.3, 25 °C. **D**, **I**, ‡, and **N** are the unfolded state, the transient intermediate, the major transition state and the native state, respectively. k_u is the unfolding rate constant corresponding to the free-energy difference between **N** and ‡, k_f is the refolding rate constant corresponding to the free-energy difference between **I** and ‡, and $k^{calc}_{D\text{-}N}$ is the refolding rate constant expected if the refolding were a two-state process **D** → **N**. $k^{calc}_{D\text{-}N}$ can be derived from k_u (Figure 4) and $\Delta G_{D\text{-}N}$ (Figure 8) by eq 8. As discussed in the text, **D** and **I** constitute the most unfolded and the most structured conformations in the preequilibrium, or even the endpoints of a continuum of denatured conformations. At pH 6.3, **I** represents the most stable denatured conformation, and the refolding reaction proceeds **I** → ‡ → **N** with an observed rate constant k_f, whereas, at low pH, **D** may become the most stable conformation in the preequilibrium and the refolding reaction proceeds **D** → ‡ → **N** with a rate constant corresponding to $k^{calc}_{D\text{-}N}$. Under conditions where both **D** and **I** are populated in the preequilibrium the observed rate constant is given by eq A1.

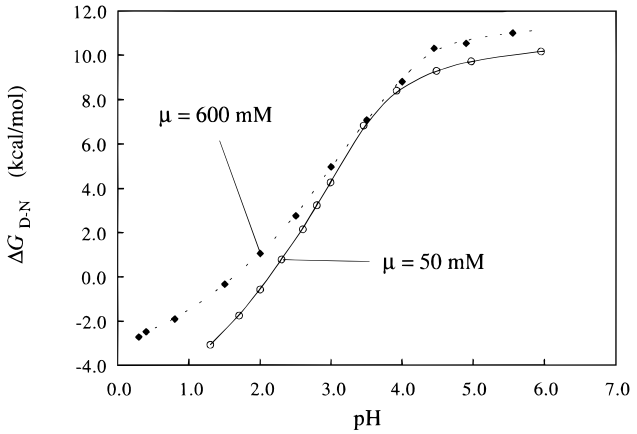

FIGURE 8: pH dependence of the stability of barnase, $\Delta G_{D\text{-}N}$, and its dependence on ionic strength. (○) $\mu = 50$ mM and (◆) $\mu =$ 600 mM. The data are obtained from CD-monitored thermal transitions (Oliveberg *et al.*, 1994).

2−3 residues titrate between pH 3 and 1.5, and at least one residue appears protected at pH 0.5 (Figure 10). It is important to point out here that the value of $\Delta Q_{D\text{-}N}$, the difference in number of protons bound to the native state and the denatured state (eq 4), may well represent the sum of fractional protonation delocalized over several interacting residues. Possible candidates for such electrostatically coupled residues with anomalous pK_A values are Asp 54, Glu 73, Asp 75, and Asp 86 (Oliveberg *et al.*, 1995). These residues are located in the positive field of the active site, closely spaced, and separated by a medium of relatively low dielectric constant [cf. Mauguen *et al.* (1982)].

By measuring ΔQ (eqs 4 and 5) it is possible to assess the degree of protection of titrating residues in the transition

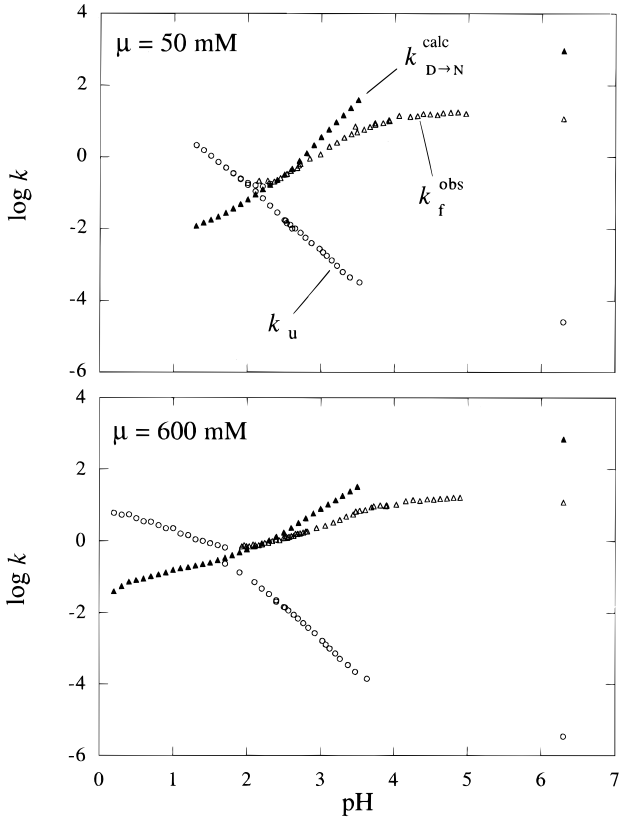

FIGURE 9: Full set of kinetics representing the acid denaturation of barnase, showing the deviation from two-state behavior. The rate constant k has units of s^{-1}. (Top panel) Observed refolding rate constant at $\mu = 50$ mM, k_f^{obs} (△), the unfolding rate constant, k_u (○); and the refolding rate constant expected for a two-state process, $k_{D\rightarrow N}^{calc}$ (▲), which represents the difference in free energy between the fully denatured state and the major transition state (cf. eq 8, Figure 7). At 25 °C, barnase displays a two-state folding process at pH values lower than ~2.5, and non-two-state behavior at higher pH values. The difference between k_f^{obs} and $k_{D\rightarrow N}^{calc}$ can be related to the equilibrium constant between **D** and **I** according to eq 9. (Bottom panel) The corresponding data set at $\mu = 600$ mM.

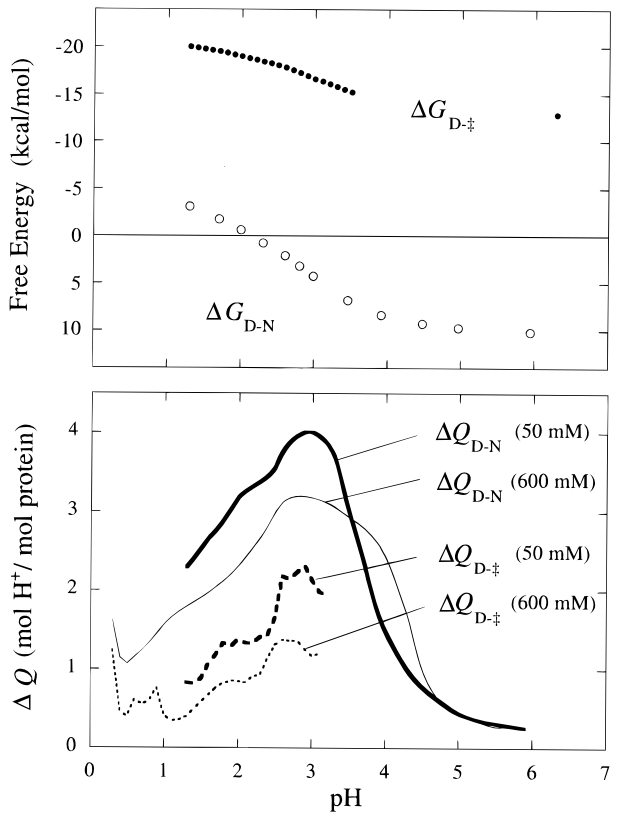

FIGURE 10: Titration behavior of the native state (**N**) and the major transition state (‡) of barnase. (Top panel) The pH dependent free energies of **N** and ‡ relative to the denatured state at $\mu = 50$ mM and 25 °C. (Lower panel) The lines show the difference in number of bound protons (ΔQ) between **N**, ‡, and the denatured state of barnase as a function of pH: (bold line) $\Delta Q_{D\text{-}N}$ at $\mu = 50$ mM and (thin line) at $\mu = 600$ mM; (dashed bold line) $\Delta Q_{D\text{-}‡}$ at $\mu = 50$ mM and (dotted thin line) at $\mu = 600$ mM. The values for ΔQ are calculated from the derivative of $\Delta G_{D\text{-}N}$ and $\Delta G_{‡\text{-}N}$ (top panel) according to eq 4. Although ΔQ decreases at high ionic strength, the difference in ΔQ between **N** and ‡ remains approximately constant.

state (‡). The degree of protection is related directly to the extent of electrostatic interactions in the protein and can be used as a structural probe by comparing with those of the native protein and the denatured state. The titration properties of the major transition state are obtained from (i) the pH dependence of the unfolding rate constant (k_u, Figure 9) which gives $\Delta G_{N\text{-}‡}$(pH) according to eq 1, (ii) the relation to the denatured state $\Delta G_{D\text{-}‡}$(pH) = $\Delta G_{D\text{-}N}$(pH) − $\Delta G_{N\text{-}‡}$(pH) (cf. Figure 7), and (iii) eq 4 which is the relation between $\Delta G_{D\text{-}‡}$(pH) and $\Delta Q_{D\text{-}‡}$(pH). The titration properties of ‡ are compared with those of the native protein in Figure 10. The result shows that, although the overall resistance to protonation is weakened, ‡ maintains a high proportion of the pK_A shifts present in the native conformation. In other words, a significant portion of the native electrostatic interactions are formed in the transition state; some of these interactions may be as strong as in the native structure—the equivalent of ~2 residues are protected at pH 3, and the transition state is still not fully protonated at pH 0.3.

Shakhnovich and Finkelstein (1989) have proposed that the **N** → ‡ transition is accompanied by an enthalphically unfavorable melting/expansion of the native structure, where the degree of swelling in the transition state does not permit rotational isomers of the side chains or penetration of water molecules. The model suggests that the interior of the transition state maintains a low dielectric constant and, hence, native-like electrostatic interactions, while the outer layers of the protein are loosened with a consequent loss of surface interactions. Our data are consistent with this model.

Extent of Structure in the Transition State. It is suggested from urea-unfolding experiments that the "degree of consolidation" of the transition state of barnase (β^u) is about 0.75 of the native protein (Figure 11). This value, which is derived from the urea dependence of the stability of ‡ and **N** ($\beta^u = (\partial\Delta G_{D\text{-}‡}/\partial[\text{urea}])/(\partial\Delta G_{D\text{-}N}/\partial[\text{urea}])$), is generally believed to constitute a measure of solvent exposure of hydrophobic residues (Tanford 1968, 1970). A similar parameter, β^{pH}, can be derived from the acid-denaturation data in Figure 10: $\beta^{pH} = (\int\Delta Q_{D\text{-}‡}\partial\text{pH})/(\int\Delta Q_{D\text{-}N}\partial\text{pH})$, i.e. the ratio of the areas under $\Delta Q_{D\text{-}‡}$ and $\Delta Q_{D\text{-}N}$. These areas are measures of the free-energy required to protonate ‡ and **N** relative to the denatured state. The value of β^{pH} is ~0.5 (Figure 11), and this would then represent a measure of the electrostatic interactions in the transition state, i.e., the degree of consolidation of electrostatic interactions. Accordingly, it may be concluded from Figure 11 that electrostatic interactions are formed, on average, later than hydrophobic interactions and are, therefore, not as important for the early folding events. However, such a conclusion could easily be misleading. If the transition state is considered to be an

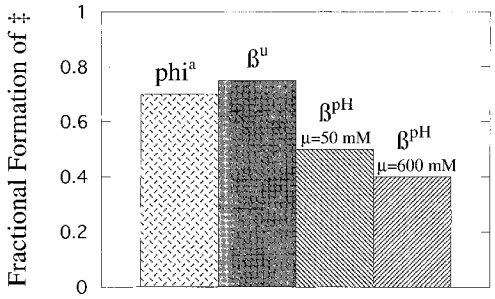

FIGURE 11: Degree of formation (the reaction coordinate) of the major transition state (‡) on the folding pathway of barnase measured by various criteria. Values of 1 and 0 represent the structures of the native state and the denatured state respectively. β^u is the degree of burial of hydrophobic residues in ‡, which has been determined by urea-denaturation experiments using the method of Tanford (see text, M.O. and A.R.F., unpublished results) and is about 0.75 of that in the native state. This value corresponds well with the average ϕ value in ‡ ($\phi = 0.7$), i.e., the extent of consolidation of intramolecular interactions in ‡ (Serrano *et al.*, 1992). β^{pH} is the extent of formation of electrostatic interactions in ‡, which is measured from ΔQ in Figure 10 (see text). β^{pH} is significantly less than β^u, about 0.5 at an ionic strength of 50 mM. The low value of β^{pH} suggests that the electrostatic interactions are lost predominantly from the surface of ‡, since, in an expanded conformation, the surface residues will be further apart than those in the (hydrophobic) interior. The effect of ionic strength on β^{pH} shows that the electrostatic interactions (charge repulsions) are more solvent accessible in ‡ than in the native protein.

expanded form of the native protein, it follows that its peripheral parts will experience, on average, a higher degree of expansion than its interior. Since most hydrophilic residues are confined to the surface of the protein, these will be, on average, less consolidated than more buried hydrophobic groups. This is expected, however, and does not monitor the strength of electrostatic interactions in more structured parts of the transition state. In fact, the highly anomalous pK_A values of ‡ suggest that the low value of β^{pH} represents the average of a few strong (key) interactions and (surface) interactions that are not yet consolidated.

Titration Behavior of the Folding Intermediate. Although the formation and unfolding of the intermediate is too fast to be determined by stopped-flow methods, its titration properties may still be determined from the refolding kinetics: the pH dependence of k_f corresponds directly to the difference in degree of protonation between the intermediate and the transition state (Figure 7). First, however, it is crucial to understand fully the behavior of the observed refolding rate constant, k_f^{obs}, which is determined not only by the free-energy difference between the intermediate and the major transition state but also by the relative occupancy of the intermediate in the preequilibrium, $C = [\mathbf{I}]/([\mathbf{I}] + [\mathbf{D}])$ (see Appendix). The stability of **I** relative to **D** ($\Delta G_{D\text{-}I}$) at pH 6.3 and 25 °C is about = 2.8 kcal/mol (eq 9 below and Table 1 in the accompanying paper), which corresponds to an occupancy of **I** in the preequilibrium of more than 99%. Accordingly, k_f^{obs} represents a good measure of k_f under these conditions ($C > 0.99$, eq A1). At lower pH values, however, where the occupancy of **I** in the preequilibrium decreases, k_f^{obs} becomes lower than expected from the free-energy difference between **I** and ‡, i.e. $k_f^{obs} \approx k_f^{app} = Ck_f$ where $C < 1$ (eq A1). Consequently, the stability of **I** cannot be measured directly from k_f^{obs} at low pH but has to be derived on the basis of assumptions about the preequilibrium (see Appendix).

To describe our results quantitatively, we use the deviation from two-state behavior to represent the apparent stability of an intermediate ($\Delta G_{D\text{-}I}^{app}$). This defined quantity can be measured directly without assumptions about the folding pathway and can be used to calculate the energetics of the components in the preequilibrium on the basis of any folding mechanism (see Appendix). Here, we calculate the equilibrium constant between **D** and **I** ($K_{D\text{-}I}$) from the minimal three-state model in Scheme 1 and Figure 7, using

$$\frac{\Delta G_{D\text{-}I}^{app}}{2.3RT} = \log k_{D\rightarrow N}^{calc} - \log k_f^{app} = \log(1 + K_{D\text{-}I}) \quad (9)$$

where $\log k_{D\rightarrow N}^{calc}$ is the refolding rate constant corresponding to the free-energy difference between **D** and ‡ (eq 8, Figure 9), and $\log k_f^{app}$ is the apparent refolding rate constant. $k_f^{app} \approx k_f^{obs}$ under the conditions at which eq 9 is applied (eq A1, Figure 9). From the pH dependence of $K_{D\text{-}I}$ it is possible to calculate $\Delta Q_{D\text{-}I}$, the difference in number of H^+ bound to **D** and **I**, respectively. The pH dependence of $\log(1 + K_{D\text{-}I})$, $\log K_{D\text{-}I}$ and $\Delta Q_{D\text{-}I}$ is shown in Figure 12. As the derivative of $\log K_{D\text{-}I}$ will be subject to an excessive error at pH values where $\log(1 + K_{D\text{-}I})$ approaches zero, $\Delta Q_{D\text{-}I}$ is shown only at pH values where $\log(1 + K_{D\text{-}I}) > 0.05$. As shown in the top panel of Figure 12, the midpoint for the **I** $\rightleftarrows$ **D** transition ($K_{D\text{-}I} = 1$) appears to be at pH 2.85 for $\mu =$ 50 mM and at pH 2.70 for $\mu = 600$ mM. However, the pH dependence obtained for $\Delta Q_{D\text{-}I}$ with eq 9 does not give sensible results (bottom panel, Figure 12): instead of decreasing at lower pH values, as **I** would be expected to become increasingly protonated, $\Delta Q_{D\text{-}I}$ apparently increases.

To explain the ambiguous behavior of **I**, we have to examine the way the experiments are performed. The analysis of the folding intermediate is indirect and relies on the equilibrium constant for unfolding ($K_{D\text{-}N}$), so any perturbation of the pH dependence of $K_{D\text{-}N}$ will be manifested in the value of $\Delta Q_{D\text{-}I}$. Since $K_{D\text{-}N}$ is derived from thermal-denaturation experiments at temperatures around 55 °C at neutral pH, and at lower temperatures (≥20 °C) under acid conditions, it is important to investigate to what extent the determination of $K_{D\text{-}N}$ is perturbed by temperature-induced changes of the denatured state [cf. Griko *et al.* (1994)]. To this end, a more extensive analysis of the intermediate is presented in the accompanying paper where the coupling between melting temperature and deviation from two-state kinetics is investigated.

The Effect of Ionic Strength on Conformational Stability. Here, the effect of solvent ions is used to investigate the localization and environment of the electrostatic interactions described above. In general, surface-exposed interactions are more affected by solvent ions than are charge interactions in poorly hydrated parts of the protein.

Accordingly, the salt-induced stabilization of the native state ($\Delta\Delta G_{D\text{-}N}^{\mu} = \Delta G_{D\text{-}N}^{\mu=600mM} - \Delta G_{D\text{-}N}^{\mu=50mM}$) relative to that of ‡, **I**, and **D** at pH values above 4 (Figure 13) is attributed to salt-accessible repulsive interactions that are exclusively present within the native fold. Although the net charge of barnase is only +3 in this pH region, the surface of the native protein shows an irregular charge distribution with one negative and two positive patches in the active site which are likely to put electrostatic strain on the structure (Meiering *et al.*, 1992). The stabilization of **N** relative to the other

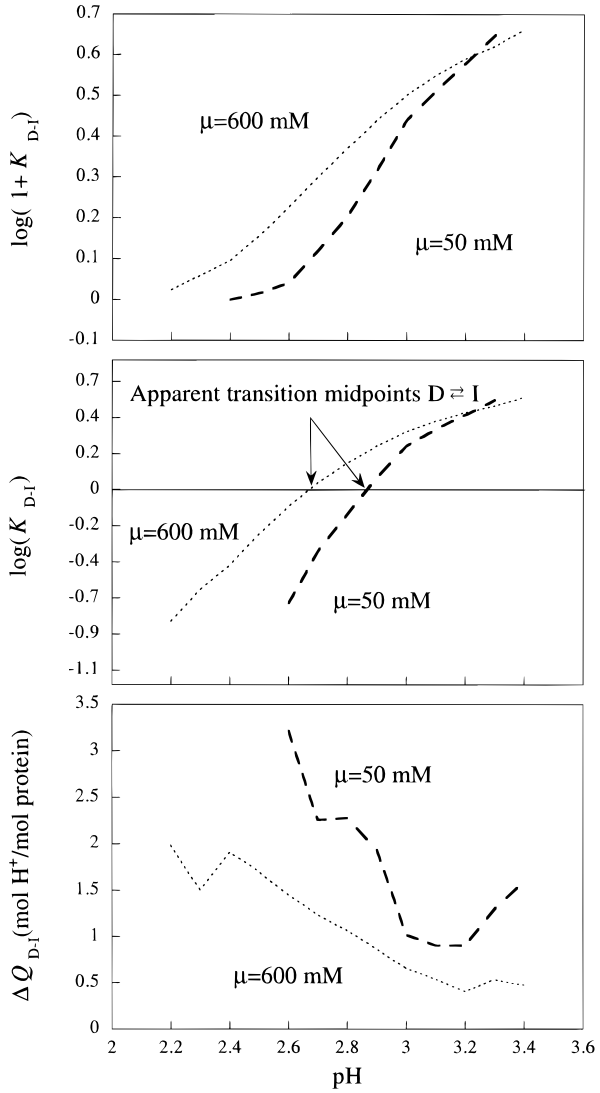

FIGURE 12: pH dependence of stability data relating to the folding intermediate of barnase. Bold broken lines, $\mu = 50$ mM. Thin dotted lines, $\mu = 600$ mM. (Top panel) The apparent stability of the intermediate relative to the denatured state, derived from the difference between the observed refolding rate constant k_f^{obs} (Figure 9) and that predicted from a two-state model $k_{D\rightarrow N}^{calc}$ (Figure 9) according to eq 9 (see text for further discussion) (Middle panel) The equilibrium constant between the folding intermediate and the denatured state (K_{D-I}) according to a three-state model. Apparently, the midpoint for the **I** ⇄ **D** transition ($K_{D-I} = 1$) takes place at pH 2.85 at $\mu = 50$ mM, and at pH 2.70 at $\mu = 600$ mM. (Bottom panel) The titration by protons of the intermediate, as calculated from $\partial \log K_{D-I}/\partial$pH (eq 4, cf. Figure 10, bottom panel). The pH dependence of ΔQ_{D-I} obtained by the three-state model appears unrealistic and is further discussed in the text.

conformations suggests that these charge patches are consolidated very late in the folding pathway.

It appears, however, that the stabilization of the native state ($\Delta\Delta G^{\mu}_{D-N}$) decreases rapidly below pH 4 and displays a minimum around pH 3.5 (Figure 13). Based on the assumption that salt counteracts (and does not enhance) the pK_A shifts, it has been suggested that the drop in $\Delta\Delta G^{\mu}_{D-N}$ is not due to effects on **N** *per se* but is caused by a salt-induced stabilization of **D** (Oliveberg *et al.*, 1994, 1995). That is, not only the native state but also the unfolded conformation involves intramolecular charge repulsions, the magnitude of which rapidly increases when it becomes protonated (the net charge increases from +4 to +17). Hence, the effect of ionic

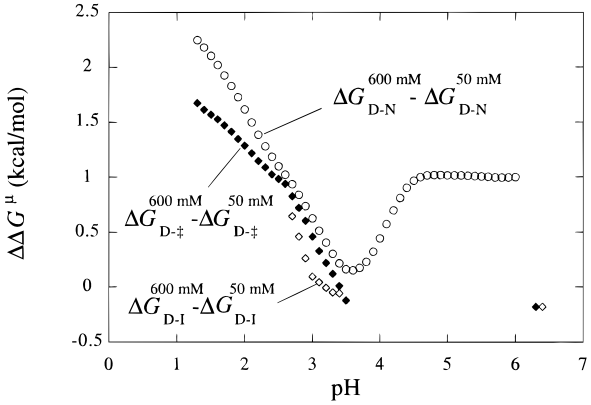

FIGURE 13: Salt-induced stabilization of the native state of barnase (○), its major transition state (◆), and the transient intermediate (◇). The plots are derived by subtracting stability data obtained at $\mu = 50$ mM from those obtained at $\mu = 600$ mM.

strength on the stability of **D** (the reference conformation) is not constant throughout the pH range but increases rapidly around pH 4, reflected by the apparent drop in $\Delta\Delta G^{\mu}_{D-N}$ (Figure 13). Below pH 3.5, $\Delta\Delta G^{\mu}_{D-N}$ displays a more or less linear increase, which reflects the titration (i.e., increasing net charge) of the native state at lower pH values (Figure 13).

Interestingly, the salt-induced stabilization of the transition state ($\Delta\Delta G^{\mu}_{D-\ddagger}$) follows that of the native state below pH 3.5 (Figure 13). This suggests that ‡ titrates in a way similar to **N** in the low-pH range, although ‡ seems to lack the repulsive interactions that give rise to the salt effect on **N** at higher pH. The result is consistent with the transition state having a loosened surface distribution of charges, but remaining compact and retaining some of the most anomalous pK_A values of the native state.

The salt effect on the stability of the intermediate ($\Delta\Delta G^{\mu}_{D-I}$) appears similar to that of the transition state. This may show that the intermediate also consists of a consolidated native-like core surrounded by a loose and extended shell structure. As with the titration properties of the folding intermediate, however, $\Delta\Delta G^{\mu}_{D-I}$ behaves ambiguously and shows an accelerating increase at lower pH values [for further discussion, see Oliveberg and Fersht (1996)].

The slight destabilization of the transition state and the intermediate (0.2−0.3 kcal/mol) which is observed above pH 4 supports further the idea of these states consisting of a mixture of denatured-like and native-like structure. Their denatured-like content is stabilised by salt according to the behavior of the denatured state, whereas their native-like fractions are less sensitive to salt and contributes therefore to a net destabilization relative to the denatured state.

CONCLUDING REMARKS

It can be concluded from this study that a significant portion of native-like electrostatic interactions are formed in the transition state and that some of these interactions are strong and give rise to native-like pK_A values: the transition state shows some highly anomalous pK_A values and is not fully protonated at pH 1. For comparison, the denatured state is fully protonated around pH 3. Taken together, however, the charge repulsions within the transition state are weaker than those of the native state. This suggests that the

transition state for unfolding is an expanded form of the native state, with a poorly solvated interior and disrupted surface regions. We are now applying the approach of this study to mutant proteins in order to characterize the electrostatic interactions in the transition state on the level of individual residues. The results referring to the folding intermediate imply that this species has many similarities with the transition state. However, these data are not conclusive on their own since they may be perturbed by temperature variations of the acid/thermally denatured state. Therefore, the properties of the folding intermediate are discussed more extensively in the accompanying paper where the temperature dependence of the ionization equilibria in this study is investigated (Oliveberg & Fersht, 1996).

ACKNOWLEDGMENT

We want to thank Dr. Jane Clarke for valuable comments on the manuscript.

APPENDIX

Effects of the Preequilibrium on the Observed Refolding Rate Constant. If it is assumed that the folding pathway involves more than one folding intermediate, say *n* intermediates,

Scheme A1

$$\mathrm{D} \overset{K_1}{\rightleftharpoons} \mathrm{I}_1 \overset{K_2}{\rightleftharpoons} \mathrm{I}_2 \rightleftarrows \ldots \rightleftarrows \mathrm{I}_{n-1} \overset{K_n}{\rightleftharpoons} \mathrm{I}_n \underset{k_u}{\overset{k_f}{\rightleftharpoons}} \mathrm{N}$$

and that the interconversion between the *n* intermediate states and the denatured state is much faster than k_f, eq 6 expands to $k^{obs} = k_f^{app} + k_u = Ck_f + k_u$ where

$$C = \frac{[\mathrm{I}_n]}{[\mathrm{D}] + \sum_{i=1}^{n}[\mathrm{I}_i]} = \frac{1}{1 + \sum_{i=1}^{n}\prod_{j=i}^{n} K_j} \qquad \text{(A1)}$$

k_f^{app} is the apparent refolding rate constant, $\mathbf{I}_n$ the intermediate immediately preceding the major transition state, and *C* the fraction ($0 < C < 1$) of denatured species I_n that accumulates in the preequilibrium. For convenience, we define the rapid preequilibrium that establishes between **D** and $\mathbf{I}_1$ to $\mathbf{I}_n$ prior to the formation of **N** as the pre(transition-state)equilibrium. To appreciate qualitatively the effect on k_f^{app} by variations in the preequilibrium, it is useful to consider the following idealized cases:

(i) Under conditions when the preequilibrium is considerably shifted toward $\mathbf{I}_n$ (or $n = 1$, Scheme 1) and the occupancy of other intermediate or denatured states is negligible, *C* approaches 1 and, thus, $k_f^{app} \approx k_f$. In this case, the free energy difference between the native state and $\mathbf{I}_n$ can be calculated directly from k_f^{app} and k_u according to a two-state process (eq 7). $\Delta G_{D\text{-}In}$ is then obtained by $\Delta G_{D\text{-}N} - \Delta G_{N\text{-}In}$ (cf. Figure 7).

(ii) If *more* than one conformation is populated during the preequilibrium, *C* in eq 8 will become smaller than 1 and, consequently, $k_f^{app} < k_f$. For example, $C = [\mathrm{I}_n]/([\mathrm{I}_n] + [\mathrm{D}])$ when no other conformations than **D** and I_n are populated (or $n = 1$, Scheme 1). In this case, $\Delta G_{N\text{-}In}$ cannot be calculated directly from the observed kinetics, but k_f^{app} has to be corrected for *C* (ie., $k_f = k_f^{app}/C$).

(iii) In a situation where there are no clear transition states (ie., no, or insignificant, free-energy barriers) between **D** and I_n, and *n* is a very large number, the system in Scheme A1 approaches a so-called *variable two-state mechanism* or second-order transition (Dill & Shortle, 1991; Griko *et al.*, 1994). In this case the term "folding intermediates" gets a slightly different meaning: the denatured state would, hence, consist of a continuum of substates, ranging from an extended random coil (under highly denaturing conditions) to a compact, partly structured species in pure water. Further, the folding events leading from an extended to more structured denatured states would not be bound to follow a strictly sequential pathway but could also proceed in a more parallel manner, where different parts of the polypeptide chain fold independently. Such second- or higher order phase transitions have been predicted for the unfolding of homopolypeptide chains whose folded state is compact but without any unique tertiary structure (Karplus & Shakhnovich, 1992) and has been experimentally supported by the noncooperative unfolding of several molten globule states (Ptitsyn, 1992). Regarding the kinetics, k_f^{app} would always represent the free energy between the most stable (ensemble of) denatured conformation(s) in the preequilibrium, $\mathbf{I}_i$, and ‡ according to eq 1. That is, the kinetics do not, as above, represent the refolding of a specific conformation, the concentration of which varies with denaturant, but rather the refolding of a full population of a denatured species the *structure* of which varies with denaturant. Thus, $\Delta G_{D\text{-}I}^{app}$(pH) is equal to the free energy difference between **D** and $\mathbf{I}_i$, where *i* varies with pH. In this case, however, $\mathbf{I}_i$ may not be a defined intermediate state but more likely an ensemble of denatured conformations which average properties is represented by $\mathbf{I}_i$ (Karplus & Shakhnovich, 1992; Griko *et al.*, 1994).

Accordingly, it is impossible to extract detailed information about the stability of folding intermediates from the refolding kinetics in the absence of knowledge about the preequilibrium.

REFERENCES

Antosiewicz, J., McCammon, J. A., & Gilson, M. K. (1994) *J. Mol. Biol. 238*, 415−436.
Bycroft, M., Matouschek, A., Kellis, J. T., Jr, Serrano, L., & Fersht, A. R. (1990) *Nature 346*, 488−490.
Creighton, T. E. (1992) in *Protein Folding* (Creighton, T. E., Ed.) pp 301−351, W. H. Freeman and Co., New York.
Dill, K. A., & Shortle, D. (1991) *Annu. Rev. Biochem. 60*, 795−825.
Finkelstein, A. V., & Shakhnovich, E. I. (1989) *Biopolymers 28*, 1681−1694.
Goto, Y., & Fink, A. L. (1989) *Biochemistry 28*, 945−952.
Goto, Y., & Nishikiori, S. (1991) *J. Mol. Biol. 222*, 679−686.
Goto, Y., Takahashi, N., & Fink, A. L. (1990) *Biochemistry 29*, 3480−3488.
Griko, Y. V., Freire, E., & Privalov, P. I. (1994) *Biochemistry 33*, 1889−1899.
Karplus, M., & Shakhnovich, E. (1992) in *Protein Folding* (Creighton, T. E., Ed.) pp 127−195, W. H. Freeman and Co., New York.
Kiefhaber, T., Kohler, H.-H., & Schmid, F. X. (1992) *J. Mol. Biol. 224*, 217−239.
Kuwajima, K. (1989) *Proteins: Struct., Funct., Genet. 6*, 87−103.
Matouschek, A., Kellis, J. T., Jr., Serrano, L., Bycroft, M., & Fersht, A. R. (1990) *Nature 346*, 440−445.
Matouschek, A., Serrano, L., & Fersht, A. R. (1992) *J. Mol. Biol. 224*, 819−835.

Matouschek, A., Matthews, J. M., Johnson, C. M., & Fersht, A. R. (1994) *Protein Eng. 7*, 1089−1095.
Mauguen, Y., Hartley, R. W., Dodson, E. J., Dodson, G. G., Bricogne, G., Chothia, C., & Jack, A. (1982) *Nature 29*, 162−164.
Meiering, E. M., Serrano, L., & Fersht, A. R. (1992) *J. Mol. Biol. 225*, 585−589.
Oliveberg, M., Arcus, V., & Fersht, A. R. (1995) *Biochemistry 34*, 9424−9433.
Oliveberg, M., & Fersht, A. R. (1996) *Biochemistry 35*, 2738−2749.
Oliveberg, M., Vuilleumier, S., & Fersht, A. R. (1994) *Biochemistry 33*, 8826−8832.
Ptitsyn, O. B. (1992) in *Protein Folding* (Creighton, T. E., Ed.) W. H. Freeman and Co., New York.
Ptitsyn, O. B., Pain, R. H., Semisotnov, G. V., Zerovnik, E., & Razgulyaev, O. I. (1990) *FEBS Lett. 12*, 20−24.
Roxby, R., & Tanford, C. (1971) *Biochemistry 10*, 3348−3352.
Sanz, J. M., & Fersht, A. R. (1993) *Biochemistry 32*, 13584−13592.
Serrano, L., & Fersht, A. R. (1989) *Nature 342*, 296−299.
Serrano, L., Matouschek, A., & Fersht, A. R. (1992) *J. Mol. Biol. 224*, 805−818.
Shakhnovich, E. I., & Finkelstein, A. V. (1989) *Biopolymers 28*, 1667−1680.
Shortle, D., & Meeker, A. K. (1986) *Proteins: Struct., Funct., Genet. 1*, 81−89.
Stigter, D., & Dill, K. A. (1990) *Biochemistry 29*, 1262−1271.
Sugihara, M., & Segawa, S. (1984) *Biopolymers 23*, 2473.
Tanford, C. (1968) *Adv. Protein Chem. 23*, 121−282.
Tanford, C. (1970) *Adv. Protein Chem. 24*, 1−95.
Thornton, J. M. (1992) in *Protein Folding* (Creighton, T. E., Ed.) pp 59−81, W. H. Freeman and Co., New York.
Warshel, A., & Åqvist, J. (1991) *Annu. Rev. Biophys. Biophys. Chem. 20*, 267−298.
Wong, K., & Hamlin, L. M. (1974) *Biochemistry 13*, 2678−2683.

BI9509661